RESEARCH ARTICLE | FEBRUARY 06 2025

# Nonreciprocal superconductivity at $Ti_2O_3$/GaN interface

Peng Dong; Lijie Wang; Guanqun Zhang; Zhongfeng Ning ; Jiadian He; Yiwen Zhang; Yifan Ding ; Xiaohui Zeng ; Yanjiang Wang; Jinghui Wang ; Xiang Zhou ; Yueshen Wu ; Wei Li ; Jun Li



*APL Quantum* 2, 016114 (2025)
https://doi.org/10.1063/5.0237619

APL Quantum ARTICLE pubs.aip.org/aip/apq

# Nonreciprocal superconductivity at $Ti_2O_3$/GaN interface

Cite as: APL Quantum 2, 016114 (2025); doi: 10.1063/5.0237619
Submitted: 5 September 2024 • Accepted: 15 January 2025 •
Published Online: 6 February 2025

View Online Export Citation CrossMark

Peng Dong,[1] Lijie Wang,[2] Guanqun Zhang,[2] Zhongfeng Ning,[2] Jiadian He,[1] Yiwen Zhang,[1] Yifan Ding,[1] Xiaohui Zeng,[1] Yanjiang Wang,[1] Jinghui Wang,[1] Xiang Zhou,[1,a)] Yueshen Wu,[1,a)] Wei Li,[2,a)] and Jun Li[1,a)]

## AFFILIATIONS

[1] ShanghaiTech Laboratory for Topological Physics and School of Physical Science and Technology, ShanghaiTech University, Shanghai 201210, China

[2] State Key Laboratory of Surface Physics and Department of Physics, Fudan University, Shanghai 200433, China

[a)] Authors to whom correspondence should be addressed: zhouxiang@shanghaitech.edu.cn; wuysh@shanghaitech.edu.cn; w_li@fudan.edu.cn; and lijun3@shanghaitech.edu.cn

## ABSTRACT

Two-dimensional superconductors exhibit intriguing quantum physical phenomena and hold promising potential for superconducting circuit applications due to their inherently broken inversion symmetry, which can introduce additional degrees of freedom related to spin or momentum. Achieving chemical stability in atomic layer 2D superconductors, including mechanical exfoliation and film deposition, remains both fundamentally and technologically challenging. Naturally, interfacial superconductivity, enclosed and safeguarded between two materials, is considered an ideal two-dimensional candidate, providing a stable and immaculate platform to explore correlated phenomena with inversion symmetry breaking in the 2D limit. Here, we report a Rashba spin–orbit coupling induced momentum-dependent superconducting order parameter in the inversion symmetry breaking heterointerface superconductor $Ti_2O_3$/GaN. Remarkably, nonlinear responses emerge in the superconducting transition regime when the magnetic field is precisely aligned parallel to the interface and perpendicular to the applied current. In particular, the observed nonreciprocal supercurrent is extremely sensitive to the direction of the field for 0.5°, suggestive of a crossover from a symmetry breaking state to a symmetric one. Our finding unveils the underlying rich physical properties in heterointerface superconductors, providing an exciting opportunity for the development of novel mesoscopic superconducting devices.





Symmetry breaking plays an essential role in the emergence of superconductivity[1–3] and influences many physical properties[4–6] in a profound way, which provides a fundamental understanding of the Cooper pair formation in superconductivity.[7–9] In conventional superconductors, a condensate of Cooper pairs spontaneously breaks only the $U(1)$ gauge symmetry.[10] In unconventional superconductors, however, additional symmetries will be further broken, giving rise to enormous novel physical behaviors and the possibility of multiple superconducting phases.[11–15] In particular, broken rotational symmetry in high-$T_c$ cuprate superconductors exhibits an anisotropic $d$-wave pairing symmetry,[16,17] and broken time-reversal symmetry in superconductivity could induce spin-triplet Cooper pairs.[18–20] Compared to the novel states induced by the spontaneous symmetry breaking of order parameter, symmetry breaking present in the normal state can also lead to the emergence of intriguing phenomena. For example, broken lattice inversion symmetry in noncentrosymmetric compounds could result in the coexistence of spin-singlet and spin-triplet pairings.[18,19] Strikingly, two-dimensional heterointerface superconductors possess a natural inversion symmetry breaking, and the existence of the interfacial electric field leads to a strong spin–orbit coupling (SOC), resulting in the mixed-parity superconductivity with an admixture of $s$-wave and $p$-wave pairings,[21–23] a candidate platform for realizing Majorana modes.[24–26] Consequently, it is pivotal to reveal the emergent of fascinating and non-trivial superconducting properties at the heterointerfaces with inversion symmetry breaking and develop next-generation quantum technologies.

To illustrate the appealing physical properties reflecting inversion symmetry breaking in lattice and electronic structures of the two-dimensional superconductors, the nonreciprocal supercurrent

(NSC), which emerges only when both inversion and time-reversal symmetries are broken,[27–31] has recently played a pivotal role in electronic transport.[32–35] A typical electronic band structure with Rashba-like SOC could be responsible for the NSC in an interfacial superconductivity of $Bi_2Te_3$/FeTe[36] and in a gate-induced two-dimensional superconductivity on the surface of $SrTiO_3$.[37] The nonlinearity of electric resistance $R_{xx}^{2\omega}$ that depends on the applied current $\boldsymbol{I}$ and the external magnetic field $\boldsymbol{B}$ is thus phenomenologically expressed as $R_{xx}^{2\omega} = R_0\gamma(\boldsymbol{B} \times \boldsymbol{P})\cdot\boldsymbol{I}$, where $\boldsymbol{P}$ is a unit vector, which characterizes the axis of the nonreciprocal effect,[36,38,39] $\gamma$ indicates the strength of the nonreciprocal transport, and $R_0$ represents the linear resistance. Moreover, it is interesting to elucidate the underlying and rich physical properties of Rashba-like systems that have been proposed theoretically,[40] including helical and chiral superconductivity.[14,41,42] The former breaks the inversion symmetry in the presence of magnetic field,[41] while the latter further spontaneously breaks the time reversal symmetry.[43] The origin of these quantum states, however, remains unclear and is under intense scrutiny in experiments. Alternatively, using state-of-the-art heterostructure engineering, we have developed an interfacial superconductivity of $Ti_2O_3$/GaN as a following of a striking quantum metallic state.[44,45] Due to the presence of the strong interfacial coupling between the Mott insulator $Ti_2O_3$ and the polar semiconductor GaN, it would be crucial to exploit the NSC behaviors inherent to the superconducting pair symmetry, offering innovative understanding of the underlying nature of the exotic heterointerface superconductivity.[46–48]

In this work, we delve into the nonreciprocity of the superconductivity in $Ti_2O_3$/GaN. The temperature and magnetic field dependence of second harmonic resistance $R_{xx}^{2\omega}$ reveals the value of nonreciprocal strength $\gamma$ as large as 12 $A^{-1}$ $T^{-1}$. In particular, only the in-plane magnetic field can induce NSC, and a slight tilt of the magnetic field beyond $\pm 0.5^\circ$ completely suppresses the nonreciprocity. Such a sensitively angular-dependent phenomenon puts a strong confinement to the origin of the symmetry breaking, which suggests a magnetic field-induced switching of underlining mechanism.

The $Ti_2O_3$ film was grown on a (0001)-oriented GaN substrate by using pulsed laser deposition in an ultrahigh vacuum chamber with a base pressure of $10^{-9}$ Torr as described in our previous report,[44] as shown in Fig. 1(a). The superconducting interface develops between the Mott insulator $Ti_2O_3$ and the wide-bandgap GaN, attributing to charge transfer from the polar GaN substrate to the $Ti_2O_3$ layer and the existence of oxygen vacancies. The polarity perpendicular to the interface leads to Rashba-type SOC and then results in a band splitting in the $\boldsymbol{k}_x$–$\boldsymbol{k}_y$ plane in $\boldsymbol{k}$ space, as shown in Figs. 1(c) and 1(d). When a magnetic field is applied along the $\boldsymbol{k}_y$ direction, the Fermi pocket will be shifted along the $\boldsymbol{k}_x$ direction due to the Zeeman energy, as illustrated in Figs. 1(e) and 1(f). As a consequence, the interplay between two helical bands with opposite modulation vectors will give rise to a nonreciprocal charge transport along the $\boldsymbol{k}_x$ direction if the order parameter transforms into a helical state,[14,49,50] as shown in Fig. 1(g). For a type-II two-dimensional superconductor, the vortex structures would appear when the out-of-plane magnetic field is adequately large as illustrated in Fig. 1(h). Then, the dominated mechanism of the critical current is changed from the depairing mechanism to the vortex motion, which restricts the nonreciprocity to in-plane fields. As a result, we are able to



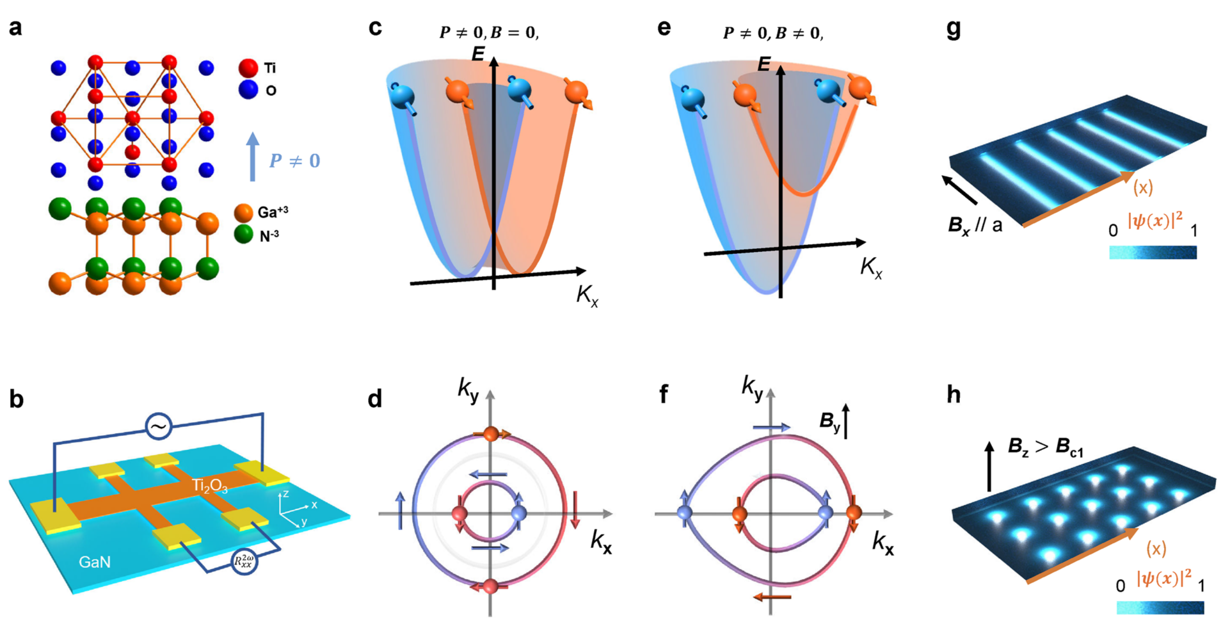


FIG. 1. Noncentrosymmetry and nonreciprocity in $Ti_2O_3$/GaN. (a) Side view and (b) Hall bar configuration of the titanium sesquioxide heterointerface $Ti_2O_3$/GaN. (c) and (e) Band structure and (d) and (f) Fermi surface of the Rashba-system induced by interface polarization with and without an in-plane magnetic field. (g) and (h) Order parameter distributions induced by applying an in-plane and an out-of-plane magnetic field, respectively. As the magnetic field is aligned in-plane, periodic order parameter in real space emerges due to the finite-momentum pairing. When the magnetic field is aligned out-of-plane, Abrikosov vortex appears.

distinguish the role of the Rashba-type SOC according to the above discussions and the relation of $R_{xx}^{2\omega} = R_0\gamma(\boldsymbol{B} \times \boldsymbol{P}) \cdot \boldsymbol{I}$.

To probe the nonreciprocal transport, a hall-bar device configuration was defined with the channel length of 300 $\mu$m and the width of 50 $\mu$m by a standard photolithography technique using a photoresist (AZ 5214) and the Ar ion beam milling (commercial Intlvac system) process to selectively remove excess materials. The nonreciprocity of the device was detected by a standard lock-in technique with four-probe geometry. All electrical measurements were performed in a Quantum Design Physical Property Measurement System (PPMS) with commercial sample rotators. The first and second harmonic resistances were defined as $R_{xx}^{\omega} = \sqrt{2}V_{xx}^{\omega}/I$ and $R_{xx}^{2\omega} = \sqrt{2}V_{xx}^{2\omega}/I$, respectively, where $I$ is the amplitude of the sinusoidal AC current source and $V_{xx}^{\omega}$ and $V_{xx}^{2\omega}$ are the amplitudes of the first and second harmonic voltages, respectively, measured using a lock-in amplifier. A phase shift of $\pi/2$ was added to the second harmonic signal.

The superconductivity and carrier profile were characterized from first harmonic resistances. In Fig. 2(a), as the temperature decreases, the longitudinal resistance $R_{xx}^{\omega}$ increases continuously until 27 K, and then, it reveals a wide range of resistance platform until a superconducting state below critical temperature $T_c$ of 4 K. Transverse hall resistance $R_{xy}^{\omega}$ (pink) under 5 T reveals a compensation of the carriers below 40 K, in agreement with the quantum metallic state in previous work.[44] The second harmonic longitudinal resistance $R_{xx}^{2\omega}$ is perceived at the superconducting transition (blue region) by applying an in-plane magnetic field of 0.5 T in Fig. 2(b). The sign of $R_{xx}^{2\omega}$ is reversed when the magnetic field is changed from 0.5 to −0.5 T, which is congruous with the field-dependent nonreciprocal signal. Nonreciprocity at 0 T was not observed, suggesting no chirality and time-reversal symmetry breaking of the superconducting order parameter.

Since the superconducting transition in the two-dimensional limit is governed by Berezinskii–Kosterlitz–Thouless (BKT) theory and thermal fluctuation above and below the mean field critical temperature $T_{c0}$, we then carefully extracted the BKT transition temperature $T_{\rm BKT}$ and $T_{c0}$ by fitting the $R$–$T$ curve with the Halperin–Nelson formula[51] (red dashed line) $R_{xx} = a \cdot e^{b\sqrt{(T_{c0}-T)/(T-T_{\rm BKT})}}$, where $a = 4\ \Omega$ is the normal state resistance, $b = -2.4$ is a dimensionless constant, $T_{\rm BKT} = 3.07 \pm 0.01$ K, and

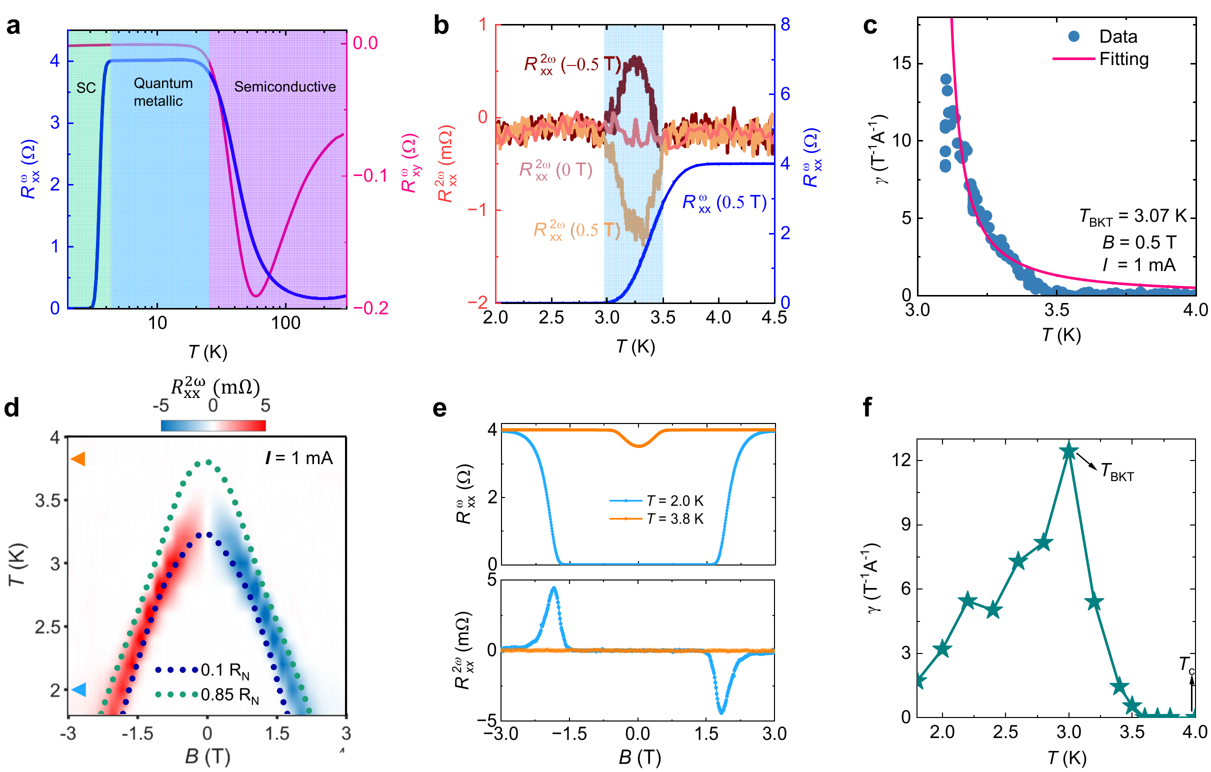


FIG. 2. Nonreciprocal charge transport as a function of magnetic field and temperature in $Ti_2O_3$/GaN. (a) Temperature-dependent longitudinal resistance $R_{xx}^{\omega}$ (blue) and transverse Hall resistance $R_{xy}^{\omega}$ (pink, under magnetic field 5 T) in $Ti_2O_3$/GaN. (b) $R_{xx}^{\omega}$ (blue) and second harmonic resistance $R_{xx}^{2\omega}$ (orange) as a function of temperature in the low temperature region, where the magnetic field and current are applied along the $y$-axis and $x$-axis, respectively. $R_{xx}^{2\omega}$ shows just a background noise under zero field and exhibits an obvious signal at the superconducting transition region under a field of 0.5 T. In particular, the sign of $R_{xx}^{2\omega}$ depends on the field as the relationship $R_{xx}^{2\omega} = R_0\gamma(\boldsymbol{B} \times \boldsymbol{P}) \cdot \boldsymbol{I}$. (c) Nonreciprocal strength $\gamma$ at fixed $\boldsymbol{B} = 0.5$ T as a function of temperature in the superconducting fluctuation region. (d) Mapping of $R_{xx}^{2\omega}$ as a function of field in temperature ranging from 1.8 to 4 K, which is antisymmetric with respect to the positive or negative field. The dashed line indicates $0.1R_N$ and $0.85R_N$ in $R_{xx}^{\omega}$, where $R_N$ is the normal state resistance at 4.5 K. (e) First and second harmonic resistance at 2 and 3.8 K, corresponding to the triangle position marked in (d). (f) Temperature-dependent nonreciprocal strength $\gamma = 2\cdot R_{xx}^{2\omega}/(BIR_{xx}^{\omega})$ at the maximum of the $R_{xx}^{2\omega}$–$\boldsymbol{B}$ at different temperatures.

$T_{c0}$ = 3.42 ± 0.03 K at 0.5 T (see Fig. S1). The nonreciprocal charge transport appears in the range of 3–3.5 K, indicative of the correlation of BKT transition or paraconductivity.[37] We evaluate the coefficient $\gamma$ representing the strength of the magnetochiral anisotropy, according to the definition of $\gamma = 2\cdot R_{xx}^{2\omega}/(BIR_{xx}^{\omega})$. Figure 2(c) shows that $\gamma$ increases as the temperature decreases. The data are fitted by the formula $\gamma = C(T - T_{\mathrm{BKT}})^{-D}$, where $C = 0.46 \pm 0.05$ A$^{-1}$ T$^{-1}$ K3$^{/2}$ and $D = 1.23 \pm 0.05$, which agrees with the BKT transition.[52] For a higher magnetic field in Fig. S2, the result is similar, and we can rule out the bulk origins of nonreciprocity due to the two-dimensional nature of the superconductivity.

We then examine the magnetic field and temperature dependences of $R_{xx}^{2\omega}$. Figure 2(d) shows the mapping of the field-dependent $R_{xx}^{2\omega}$ in various temperatures, where most of the nonreciprocal signals located in the contour of $R = 0.1\ R_{\mathrm{N}}$ and $R = 0.85\ R_{\mathrm{N}}$ (dashed lines), where $R_{\mathrm{N}}$ is the normal resistance at 4.5 K, and the raw data are presented in Fig. S4. The temperature dependence of maximum $R_{xx}^{2\omega}$ in the $R$–$H$ curves and $\gamma$ at maximum $R_{xx}^{2\omega}$ is calculated in Fig. 2(f). The maximum value of the $\gamma$ peak at 3 K is about 12 A$^{-1}$ T$^{-1}$, which is much larger than those reported previously in other heterostructures, such as Rashba semiconductor GeTe (~10$^{-3}$ A$^{-1}$ T$^{-1}$),[53] chiral organic materials (~10$^{-2}$ A$^{-1}$ T$^{-1}$),[54] BiTeBr (~1 A$^{-1}$ T$^{-1}$),[55] and $Bi_2Te_3$/FeTe interfacial superconductor (~10$^{-3}$ A$^{-1}$ T$^{-1}$),[36] while less than the noncentrosymmetric layered superconductors (~10$^{3}$ A$^{-1}$ T$^{-1}$)[22,33] and the noncentrosymmetric oxide heterointerface $LaAlO_3/SrTiO_3$ (~10$^{2}$ A$^{-1}$ T$^{-1}$).[56] It is worth noting that the suppression of the coefficient $\gamma$ at lower temperatures does not agree with the ratchet effect of vortex flow, which gives a monotonic increase in $\gamma$.[57] This is consistent with the theoretical calculation of finite-momentum pairing because one helical band begins to dominate the other as the critical field increases[49] and will be discussed further below. The nonreciprocal signal may be too weak to observe above $T_c$ for the current setup, as shown in Fig. S5.

Figures 3(a) and S6 show the magnetic field dependence of $R_{xx}^{2\omega}$ and $R_{xx}^{\omega}$ for various values of applied current $I$, which increases with current up to 4 mA and then decreases as the strength of the current is further increased. We extract the maximum value of $R_{xx}^{2\omega}$ as a function of current and plot in Fig. 3(b). The $R_{xx}^{2\omega}$ exhibits a linear increase with $I$ below 4 mA, consistent with the current-dependent $R_{xx}^{2\omega}$. Subsequently, $R_{xx}^{2\omega}$ decreases when applying a larger current, reflecting the suppression of superconductivity due to the larger current density. These characteristics indicate that the nonreciprocal signal satisfies the relation of $R_{xx}^{2\omega} \propto BI$ in the superconducting transition region.

The red and blue lines in Fig. 4(a) represent second harmonic magnetoresistances with $B$ parallel to the $z$-axis and $y$-axis, respectively, as schematically illustrated in the inset of this figure. The nonreciprocal response is almost imperceptible when the magnetic field is aligned with the $z$-axis. The results effectively eliminate the possibility of the out-of-plane Meissner screening and vortex ratchet effect.[58–60] The Meissner effect induces two non-dissipative shielding current densities on both sides when the magnetic field is aligned along the $z$-axis. The shielding currents are either added to or subtracted from the applied current on the opposite side, resulting in a corrected measured value. Thanks to the absence of out-of-plane field-induced nonreciprocity, the only effective field is the in-plane component, and a sinusoidal angular dependence is expected when the magnetic field rotates in the $yz$-plane.

Surprisingly, the angular dependence of $R_{xx}^{2\omega}$ reveals two sharp spikes instead of a sinusoidal curve as shown in Figs. 4(b) and S7. Here, the angle $\varphi$ is defined as the angle in the $yz$-plane, measured from the $z$-axis, as illustrated in the inset of Fig. 4(b). The spikes located exactly at the position where $R_{xx}^{\omega}$ reaches minimum. This phenomenon does not change with temperature and magnetic field (Fig. S7). We also conducted measurements of the magnetic field dependence of the second harmonic magnetoresistance within the range of ±1.5° near $\varphi = 90°$, as shown in Fig. 4(c). The peaks of $R_{xx}^{2\omega}$ were observed when $\varphi$ ranges from 89.7° to 90.3°. Notably, the signal disappears completely when $\varphi = 89°$ and $\varphi = 91°$. The dashed lines indicate the transition region extracted from Fig. S8.

Moreover, we measured the angular dependence of magnetoresistance in the $xz$-plane, with $\theta$ defined as the angle in the $xz$-plane measured from the $z$-axis, as depicted in the inset of Fig. 4(d). The angular-dependent $R_{xx}^{\omega}$ exhibits a twofold symmetry, with its maximum and minimum occurring at 0° and 90°, respectively. However, the $R_{xx}^{2\omega}$ signal disappears completely, suggesting that the magnetic field in the $xz$-plane does not contribute to the nonreciprocity but only superconducting suppression.

The angular dependence of $R_{xx}^{2\omega}$ seems violated the relation of $R_{xx}^{2\omega} = R_0\gamma(\boldsymbol{B} \times \boldsymbol{P})\cdot\boldsymbol{I}$, where the effective in-plane component of the magnetic fields contributes to the NSC, resulting in a sinusoidal relation for angular-dependent $R_{xx}^{2\omega}(\theta)$. Our present results are, how-



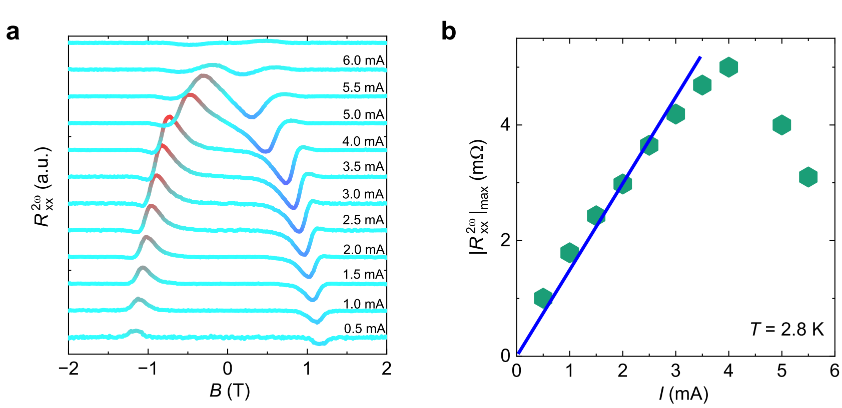


**FIG. 3.** Nonreciprocal charge transport as a function of magnetic field in various current values in $Ti_2O_3$/GaN. (a) The second harmonic signal $R_{xx}^{2\omega}$ as a function of magnetic field at different currents ranging from 0.5 to 6 mA exhibits an antisymmetric behavior about the positive and negative fields for currents $I$ < 6 mA at 2.8 K. (b) Maximum value of $R_{xx}^{2\omega}$ at $T$ = 2.8 K as a function of current $I$ extracted from (a). The blue solid line indicates the linear increase as a function of $I$ below 4 mA.

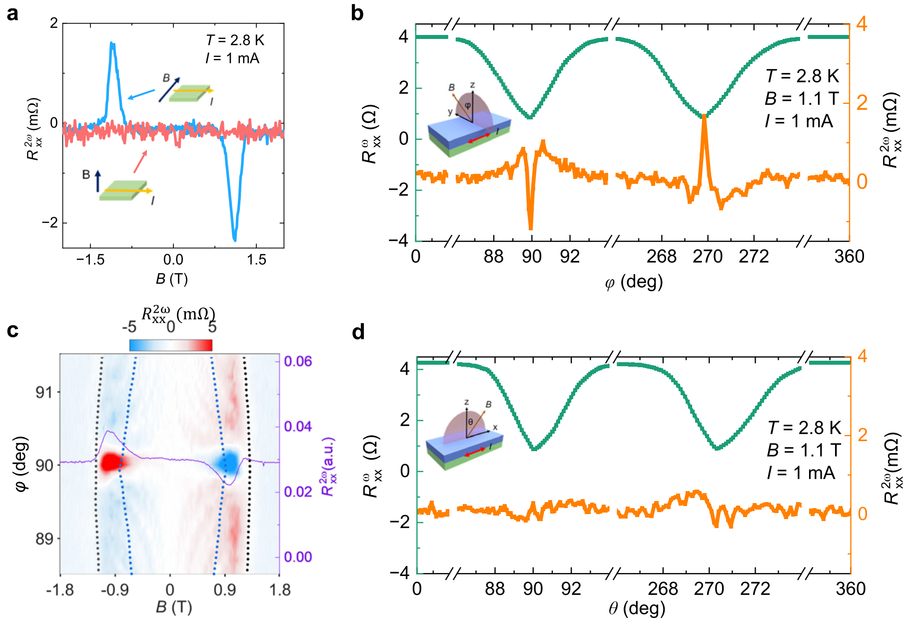


**FIG. 4.** Angular-dependent nonreciprocal charge transport in $Ti_2O_3$/GaN. (a) Field-dependent $R_{xx}^{2\omega}$ represents strong anisotropy when the direction of magnetic field is applied along the *y*-axis and *z*-axis under the condition of 1.1 T and 2.8 K. (b) Angular-dependent $R_{xx}^{\omega}$ and $R_{xx}^{2\omega}$ by rotating the magnetic fields along the *yz*-plane. The $R_{xx}^{\omega}(\theta)$ reveals a twofold symmetry with maximum and minimum at 0° and 90° (green line), respectively. $R_{xx}^{2\omega}(\theta)$ (orange line) shows a spiking anisotropy as well, which exists in an extremely narrow angle region of about ±0.5°, and represents an antisymmetric sign reversal from 90° to 270° under the condition of 1.1 T and 2.8 K. (c) Mapping of field- and angular-dependent $R_{xx}^{2\omega}$ under the condition of 2.8 K, where the field is rotated within the *yz*-plane. $R_{xx}^{2\omega}$ exists within a narrow angle region of ±0.5°, consistent with (b). The purple line represents $R_{xx}^{2\omega}$ as a function of field in $\varphi = 90°$, which is antisymmetric with respect to the positive or negative field. The dashed line (black and blue) indicates 0.1 $R_N$ and 0.85 $R_N$ in $R_{xx}^{\omega}$, where $R_N$ is the normal state resistance at 4.5 K. (d) Angular-dependent $R_{xx}^{\omega}$ and $R_{xx}^{2\omega}$ by rotating the field within the *xz*-plane. The $R_{xx}^{\omega}$ indicates a normal superconducting suppression from the effective field, while $R_{xx}^{2\omega}$ is absent.

ever, an extremely sensitive angular-dependent $R_{xx}^{2\omega}(\theta)$, suggestive of a crossover to a symmetric state in the presence of out-of-plane magnetic field. We attribute this crossover to a competition between the depairing current and the vortex depinning one,[50,61,62] as discussed in Figs. 1(g) and 1(h). In addition, we also observe a violation of the two-dimensional Tinkham-like angular dependence of critical fields from 89° to 91°, where the critical fields are slightly less than those theoretically predicted by the two-dimensional Tinkham formula (Fig. S9). When the angle is tilted, Abrikosov vortices enter the device, making the depairing energy larger than the depinning energy. The interplay between the vortex and finite momentum pairing has been discussed recently.[63] As the vortex motion does not contribute to nonreciprocity, as shown in Fig. 4(a), the second harmonic signal disappeared. Only the depairing mechanisms of superconductivity are needed to be considered. The nonreciprocity of the depairing critical current could be induced by finite momentum pairing states. It seems that our results are consistent with the theoretical prediction of helical states, as shown before.[49] However, experimental evidence of helical superconductors has been rare and challenging to observe so far. For this work, the limitation of nonreciprocal transport measurement is that it primarily appears in the superconducting fluctuation region, which has not fully transitioned into the superconducting state. The BKT transition in a noncentrosymmetric superconductor could also induce the nonreciprocity in the fluctuation region.[52] To claim the existence of helical superconductivity, further experiments are needed, such as the Josephson effect with a conventional Bardeen–Cooper–Schrieffer (BCS) superconductor.

In summary, our investigation focuses on understanding the nonreciprocity observed in the interfacial superconductor $Ti_2O_3$/GaN. The temperature and magnetic field dependences of $R_{xx}^{2\omega}$ indicate that the nonreciprocal strength $\gamma$ is as large as 12 $A^{-1}\,T^{-1}$. Furthermore, the temperature and current dependences of $R_{xx}^{2\omega}$ exhibit similar trends, wherein an initial increase is followed by a subsequent decrease as the temperature or current rises. The angular dependence of $R_{xx}^{2\omega}$ reveals that the spikes, which coincide with the point where $R_{xx}^{\omega}$ reaches its minimum, are associated with two-dimensional superconductivity. It is possible that the symmetry breaking is a consequence of nontrivial pairing.

See the supplementary material for the second harmonic resistance under different conditions, DC measurements, raw data of the first and second harmonic resistances, sample reproducibility, and angular-dependent second harmonic resistance.

This research was supported in part by the Ministry of Science and Technology (MOST) of China (Grant No. 2022YFA1603903), the National Natural Science Foundation of China (Grant Nos. 12104302, 12104303, and 11927807), the Science and Technology Commission of Shanghai Municipality (Grant No. 23ZR1404600), the Shanghai Leading Talent Program of Eastern Talent Plan, and the Double First-Class Initiative Fund of ShanghaiTech University.

## AUTHOR DECLARATIONS

### Conflict of Interest

The authors have no conflicts to disclose.

### Author Contributions

P.D. and L.W. contributed equally to this work. J.L. conceived the project. P.D. and Y.W. designed the experiments and performed the measurements. L.W. grew the sample. P.D., Y.W., J.L., and W.L. wrote the paper. All authors discussed the results and gave approval to the final version of the manuscript.

**Peng Dong**: Data curation (lead); Formal analysis (lead); Methodology (lead); Writing – original draft (lead). **Lijie Wang**: Data curation (lead). **Guanqun Zhang**: Data curation (supporting). **Zhongfeng Ning**: Data curation (supporting). **Jiadian He**: Data curation (supporting). **Yiwen Zhang**: Data curation (supporting). **Yifan Ding**: Data curation (supporting). **Xiaohui Zeng**: Data curation (supporting). **Yanjiang Wang**: Data curation (supporting). **Jinghui Wang**: Data curation (supporting). **Xiang Zhou**: Data curation (supporting). **Yueshen Wu**: Data curation (lead); Formal analysis (lead); Funding acquisition (lead); Writing – original draft (lead). **Wei Li**: Conceptualization (lead); Funding acquisition (lead). **Jun Li**: Conceptualization (lead); Data curation (lead); Formal analysis (lead); Funding acquisition (lead); Investigation (lead); Methodology (lead).

## DATA AVAILABILITY

The data that support the findings of this study are available from the corresponding author upon reasonable request.

## REFERENCES

[1] T. Hartke, B. Oreg, C. Turnbaugh, N.-Y. Jia, and M. Zwierlein, "Direct observation of nonlocal fermion pairing in an attractive Fermi–Hubbard gas," Science **381**, 82–86 (2023).
[2] H. R. Ji, Y. Liu, Y. N. Li, X. Ding, Z. Y. Xie, C. C. Ji, S. C. Qi, X. Y. Gao, M. H. Xu, and P. Gao, "Rotational symmetry breaking in superconducting nickelate $Nd_{0.8}Sr_{0.2}NiO_2$ films," Nat. Commun. **14**, 7115 (2023).
[3] C. C. Tsuei and J. R. Kirtley, "Pairing symmetry in cuprate superconductors," Rev. Mod. Phys. **72**, 969–1016 (2000).
[4] Y. Zhang, Y. H. Gu, P. F. Li, J. P. Hu, and K. Jiang, "General theory of Josephson diodes," Phys. Rev. X. **12**, 041013 (2022).
[5] K. Jiang and J. P. Hu, "Superconducting diode effects," Nat. Phys. **18**, 1145–1146 (2022).
[6] M. H. Hamidian, S. D. Edkins, C. K. Kim, J. C. Davis, A. P. Mackenzie, H. Eisaki, S. Uchida, M. J. Lawler, E. A. Kim, S. Sachdev, and K. Fujita, "Atomic-scale electronic structure of the cuprate *d*-symmetry form factor density wave state," Nat. Phys. **12**, 150–156 (2016).
[7] I. Božović and J. Levy, "Pre-formed Cooper pairs in copper oxides and $LaAlO_3$–$SrTiO_3$ heterostructures," Nat. Phys. **16**, 712–717 (2020).
[8] M. Valentini, O. Sagi, L. Baghumyan, T. de Gijsel, J. Jung, S. Calcaterra, A. Ballabio, J. Aguilera Servin, K. Aggarwal, M. Janik *et al.*, "Parity-conserving Cooper-pair transport and ideal superconducting diode in planar germanium," Nat. Commun. **15**, 169 (2024).
[9] Q.-Z. Wang, S. L. D. Ten Haaf, I. Kulesh, D. Xiao, C. Thomas, M. J. Manfra, and S. Goswami, "Triplet correlations in Cooper pair splitters realized in a two-dimensional electron gas," Nat. Commun. **14**, 4876 (2023).
[10] J. Bardeen, L. N. Cooper, and J. R. Schrieffer, "Theory of superconductivity," Phys. Rev. **108**, 1175 (1957).
[11] M. Sigrist and K. Ueda, "Phenomenological theory of unconventional superconductivity," Rev. Mod. Phys. **63**, 239–311 (1991).
[12] X. X. Wu, T. Schwemmer, T. Müller, A. Consiglio, G. Sangiovanni, D. Di Sante, Y. Iqbal, W. Hanke, A. P. Schnyder, M. M. Denner *et al.*, "Nature of unconventional pairing in the kagome superconductors $AV_3Sb_5(A = K, Rb, Cs)$," Phys. Rev. Lett. **127**, 177001 (2021).
[13] P. Dong, X.-F. Hou, J.-D. He, Y.-W. Zhang, Y.-F. Ding, X.-H. Zeng, J.-H. Wang, Y.-S. Wu, K.-J. Watanabe, T. Taniguchi, W. Xia, Y.-F. Guo, Y.-L. Chen, X. Zhou, W. Li, and J. Li, "Proximity-effect-induced superconductivity in a van der Waals heterostructure consisting of a magnetic topological insulator and a conventional superconductor," Phys. Rev. B **109**, L140503 (2024).
[14] N. F. Q. Yuan and L. Fu, "Supercurrent diode effect and finite-momentum superconductors," Proc. Natl. Acad. Sci. U. S. A. **119**, e2119548119 (2022).
[15] H. Y. Xue, L. J. Wang, Z. J. Wang, G. Q. Zhang, W. Peng, S. W. Wu, C.-L. Gao, Z. H. An, Y. Chen, and W. Li, "Fourfold symmetric superconductivity in spinel oxide $LiTi_2O_4$ (001) thin films," ACS Nano **16**, 19464–19471 (2022).
[16] Z.-X. Shen, D. S. Dessau, B. O. Wells, D. M. King, W. E. Spicer, A. J. Arko, D. Marshall, L. W. Lombardo, A. Kapitulnik, P. Dickinson *et al.*, "Anomalously large gap anisotropy in the *a-b* plane of $Bi_2Sr_2CaCu_2O_{8+\delta}$," Phys. Rev. Lett. **70**, 1553 (1993).
[17] C. C. Tsuei, J. R. Kirtley, C. C. Chi, L. S. Yu-Jahnes, A. Gupta, T. Shaw, J. Z. Sun, and M. B. Ketchen, "Pairing symmetry and flux quantization in a tricrystal superconducting ring of $YBa_2Cu_3O_{7-\delta}$," Phys. Rev. Lett. **73**, 593 (1994).
[18] A. D. Hillier, J. Quintanilla, and R. Cywinski, "Evidence for time-reversal symmetry breaking in the noncentrosymmetric superconductor $LaNiC_2$," Phys. Rev. Lett. **102**, 117007 (2009).
[19] T. Shang, M. Smidman, S. K. Ghosh, C. Baines, L. J. Chang, D. J. Gawryluk, J. A. T. Barker, R. P. Singh, D. M. Paul, G. Balakrishnan *et al.*, "Time-reversal symmetry breaking in Re-based superconductors," Phys. Rev. Lett. **121**, 257002 (2018).
[20] Z. F. Ning, J. H. Qian, Y. X. Liu, F. Chen, M. Z. Zhang, L. W. Deng, X. L. Yuan, Q. Q. Ge, H. Jin, G. Q. Zhang, W. Peng, S. Qiao, G. Mu, Y. Chen, and W. Li, "Coexistence of ferromagnetism and superconductivity at $KTaO_3$ heterointerfaces," Nano Lett. **24**, 7134 (2024).
[21] V. Kozii and L. Fu, "Odd-parity superconductivity in the vicinity of inversion symmetry breaking in spin–orbit-coupled systems," Phys. Rev. Lett. **115**, 207002 (2015).
[22] E. Zhang, X. Xu, Y. C. Zou, L. F. Ai, X. Dong, C. Huang, P. L. Leng, S. S. Liu, Y. D. Zhang, Z. H. Jia *et al.*, "Nonreciprocal superconducting $NbSe_2$ antenna," Nat. Commun. **11**, 5634 (2020).
[23] G. Q. Zhang, L. J. Wang, J. H. Wang, G. A. Li, G. Y. Huang, G. Yang, H. Y. Xue, Z. F. Ning, Y. S. Wu, J. P. Xu, Y. Song, Z. An *et al.*, "Spontaneous rotational symmetry breaking in $KTaO_3$ heterointerface superconductors," Nat. Commun. **14**, 3046 (2023).
[24] A. C. Potter and P. A. Lee, "Engineering a $p + ip$ superconductor: Comparison of topological insulator and Rashba spin–orbit-coupled materials," Phys. Rev. B **83**, 187520 (2011).
[25] Y.-Z. Liu, H. Watanabe, and N. Nagaosa, "Emergent magnetomultipoles and nonlinear responses of a magnetic hopfion," Phys. Rev. Lett. **129**, 267201 (2022).
[26] B. Lu, S. Ikegaya, P. Burset, Y. Tanaka, and N. Nagaosa, "Tunable Josephson diode effect on the surface of topological insulators," Phys. Rev. Lett. **131**, 096001 (2023).
[27] F. Ando, Y. Miyasaka, T. Li, J. Ishizuka, T. Arakawa, Y. Shiota, T. Moriyama, Y. Yanase, and T. Ono, "Observation of superconducting diode effect," Nature **584**, 373–376 (2020).
[28] H. Narita, J. Ishizuka, R. Kawarazaki, D. Kan, Y. Shiota, T. Moriyama, Y. Shimakawa, A. V. Ognev, A. S. Samardak, Y. Yanase, and T. Ono, "Field-free superconducting diode effect in noncentrosymmetric superconductor/ferromagnet multilayers," Nat. Nanotechnol. **17**, 823–828 (2022).
[29] L. Bauriedl, C. Bäuml, L. Fuchs, C. Baumgartner, N. Paulik, J. M. Bauer, K.-Q. Lin, J. M. Lupton, T. Taniguchi, K. J. Watanabe *et al.*, "Supercurrent diode

effect and magnetochiral anisotropy in few-layer $NbSe_2$," Nat. Commun. **13**, 4266 (2022).
[30]H. Wu, Y.-J. Wang, Y. F. Xu, P. K. Sivakumar, C. Pasco, U. Filippozzi, S. S. P. Parkin, Y.-J. Zeng, T. McQueen, and M. N. Ali, "The field-free Josephson diode in a van der Waals heterostructure," Nature **604**, 653–656 (2022).
[31]J. J. He, Y. Tanaka, and N. Nagaosa, "The supercurrent diode effect and nonreciprocal paraconductivity due to the chiral structure of nanotubes," Nat. Commun. **14**, 3330 (2023).
[32]Y.-W. Zhang, J.-L. Cai, P. Dong, J.-D. He, Y.-F. Ding, J.-H. Wang, X. Zhou, K. C. Cao, Y. S. Wu, and J. Li, "Intrinsic supercurrent diode effect in $NbSe_2$ nanobridge," Microstructures **4**, 2024018 (2024).
[33]R. Wakatsuki, Y. Saito, S. Hoshino, Y. M. Itahashi, T. Ideue, M. Ezawa, Y. Iwasa, and N. Nagaosa, "Nonreciprocal charge transport in noncentrosymmetric superconductors," Sci. Adv. **3**, e1602390 (2017).
[34]Y.-Y. Lyu, J. Jiang, Y.-L. Wang, Z.-L. Xiao, S. N. Dong, Q.-H. Chen, M. V. Milošević, H.-B. Wang, R. Divan, J. E. Pearson *et al.*, "Superconducting diode effect via conformal-mapped nanoholes," Nat. Commun. **12**, 2703 (2021).
[35]Y.-S. Wu, Q. Wang, X. Zhou, J.-H. Wang, P. Dong, J.-D. He, Y.-F. Ding, B.-L. Teng, Y.-W. Zhang, Y.-F. Li, C. Zhao *et al.*, "Nonreciprocal charge transport in topological kagome superconductor $CsV_3Sb_5$," npj Quantum Mater. **7**, 105 (2022).
[36]K. Yasuda, H. Yasuda, T. Liang, R. Yoshimi, A. Tsukazaki, K. S. Takahashi, N. Nagaosa, M. Kawasaki, and Y. Tokura, "Nonreciprocal charge transport at topological insulator/superconductor interface," Nat. Commun. **10**, 2734 (2019).
[37]Y. M. Itahashi, T. Ideue, Y. Saito, S. Shimizu, T. Ouchi, T. Nojima, and Y. Iwasa, "Nonreciprocal transport in gate-induced polar superconductor $SrTiO_3$," Sci. Adv. **6**, eaay9120 (2020).
[38]Y. Tokura and N. Nagaosa, "Nonreciprocal responses from non-centrosymmetric quantum materials," Nat. Commun. **9**, 3740 (2018).
[39]N. Nagaosa and Y. Yanase, "Nonreciprocal transport and optical phenomena in quantum materials," Annu. Rev. Condens. Matter Phys. **15**, 63–83 (2024).
[40]J. J. He, Y. Tanaka, and N. Nagaosa, "A phenomenological theory of superconductor diodes," New J. Phys. **24**(5), 053014 (2022).
[41]R. P. Kaur, D. F. Agterberg, and M. Sigrist, "Helical vortex phase in the noncentrosymmetric $CePt_3Si$," Phys. Rev. Lett. **94**, 137002 (2005).
[42]K. Michaeli, A. C. Potter, and P. A. Lee, "Superconducting and ferromagnetic phases in $SrTiO_3/LaAlO_3$ oxide interface structures: Possibility of finite momentum pairing," Phys. Rev. Lett. **108**, 117003 (2012).
[43]C. Guo, C. Putzke, S. Konyzheva, X. W. Huang, M. Gutierrez-Amigo, I. Errea, D. Chen, M. G. Vergniory, C. Felser, M. H. Fischer, T. NeuPert, and P. J. W. Moll, "Switchable chiral transport in charge-ordered kagome metal $CsV_3Sb_5$," Nature **611**, 461–466 (2022).
[44]L. J. Wang, W. H. He, G. Y. Huang, H. Y. Xue, G. Q. Zhang, G. Mu, S. W. Wu, Z. H. An, C. L. Zheng, Y. Chen, and W. Li, "Two-dimensional superconductivity at the titanium sesquioxide heterointerface," ACS Nano **16**, 16150–16157 (2022).
[45]G. Zhang, Y. Liu, G. Li, J. Wang, Y. Wu, L. Wang *et al.*, "Unique quantum metallic state in $Ti_2O_3$/GaN," ACS Appl. Electron. Mater. **6**, 7915–7922 (2024).
[46]P. Fulde and R. A. Ferrell, "Superconductivity in a strong spin-exchange field," Phys. Rev. **135**, A550–A563 (1964).
[47]A. I. Larkin and Y. N. Ovchinnikov, "Nonuniform state of superconductors," Sov. Phys. JETP **20**, 762 (1965).
[48]P. Wan, O. Zheliuk, N. F. Q. Yuan, X. L. Peng, L. Zhang, M. P. Liang, U. Zeitler, S. Wiedmann, N. E. Hussey, T. T. M. Palstra, and J. T. Ye, "Orbital Fulde–Ferrell–Larkin–Ovchinnikov state in an Ising superconductor," Nature **619**, 46–51 (2023).
[49]S. Ilić and F. S. Bergeret, "Theory of the supercurrent diode effect in Rashba superconductors with arbitrary disorder," Phys. Rev. Lett. **128**, 177001 (2022).
[50]A. Daido, Y. Ikeda, and Y. Yanase, "Intrinsic superconducting diode effect," Phys. Rev. Lett. **128**, 037001 (2022).
[51]B. I. Halperin and D. R. Nelson, "Resistive transition in superconducting films," J. Low Temp. Phys. **36**, 599–616 (1979).
[52]S. Hoshino, R. Wakatsuki, K. Hamamoto, and N. Nagaosa, "Nonreciprocal charge transport in two-dimensional noncentrosymmetric superconductors," Phys. Rev. B **98**, 054510 (2018).
[53]Y. Li, Y. Li, P. Li, B. Fang, X. Yang, Y. Wen, D.-X. Zheng, C.-H. Zhang, X. He, A. Manchon *et al.*, "Nonreciprocal charge transport up to room temperature in bulk Rashba semiconductor α-GeTe," Nat. Commun. **12**, 540 (2021).
[54]F. Pop, P. Auban-Senzier, E. Canadell, G. L. J. A. Rikken, and N. Avarvari, "Electrical magnetochiral anisotropy in a bulk chiral molecular conductor," Nat. Commun. **5**, 3757 (2014).
[55]T. Ideue, K. Hamamoto, S. Koshikawa, M. Ezawa, S. Shimizu, Y. Kaneko, Y. Tokura, N. Nagaosa, and Y. Iwasa, "Bulk rectification effect in a polar semiconductor," Nat. Phys. **13**, 578–583 (2017).
[56]D. S. Choe, M. J. Jin, S. I. Kim, H.-J. Choi, J.-H. Jo, I. Oh, J.-M. Park, H.-S. Jin, H.-C. Koo, B.-C. Min, S.-M. Hong, H.-W. Lee, S.-H. Baek, and J.-W. Yoo, "Gate-tunable giant nonreciprocal charge transport in noncentrosymmetric oxide interfaces," Nat. Commun. **10**, 4510 (2019).
[57]Y. M. Itahashi, Y. Saito, T. Ideue, T. Nojima, and Y. Iwasa, "Quantum and classical ratchet motions of vortices in a two-dimensional trigonal superconductor," Phys. Rev. Res. **2**, 023127 (2020).
[58]T. Le, Z.-M. Pan, Z.-K. Xu, J.-J. Liu, J.-L. Wang, Z.-F. Lou, X. Yang, Z. Wang, Y. Yao, C. Wu, and X. Lin, "Superconducting diode effect and interference patterns in kagome $CsV_3Sb_5$," Nature **630**, 64–69 (2024).
[59]D. Suri, A. Kamra, T. N. G. Meier, M. Kronseder, W. Belzig, C. H. Back, and C. Strunk, "Non-reciprocity of vortex-limited critical current in conventional superconducting micro-bridges," Appl. Phys. Lett. **121**, 10 (2022).
[60]A. Gutfreund, H. Matsuki, V. Plastovets, A. Noah, L. Gorzawski, N. Fridman, G. Yang, A. Buzdin, O. Millo, J. W. A. Robinson, and Y. Anahory, "Direct observation of a superconducting vortex diode," Nat. Commun. **14**, 1630 (2023).
[61]M. Nadeem, M. S. Fuhrer, and X. Wang, "The superconducting diode effect," Nat. Rev. Phys. **5**, 558–577 (2023).
[62]I. K. Liu, S. B. Prasad, A. W. Baggaley, C. F. Barenghi, T. S. Wood, and J. Low, "Vortex depinning in a two-dimensional superfluid," J. Low Temp. Phys. **215**, 376–396 (2024).
[63]A. Devarakonda, T. Suzuki, S. Fang, J. Zhu, D. Graf, M. Kriener, L. Fu, E. kaxiras, and J. G. Checkelsky, "Signatures of bosonic Landau levels in a finite-momentum superconductor," Nature **599**, 51–56 (2021).